Electron Tunneling through Water Layers: Effect of Polarizability

Alex Mosyak,[†] Peter Graf, Ilan Benjamin,[‡] and Abraham Nitzan*

School of Chemistry, The Raymond and Beverly Sackler Faculty of Science, Tel Aviv University, Tel Aviv 69978, Israel

Received: June 13, 1996[⊗]

In a recent work (Mosyak, A.; et al. *J. Chem. Phys.* **1996**, *104*, 1549), we investigated numerically electron tunneling through water layers confined between two solid walls. In the present paper, the effect of some of our model assumptions and parameters on the tunneling behavior is studied. In particular, we focus on the role played by the water electronic polarizability. We find that the tunneling behavior computed with water configurations prepared with a polarizable SPC water model is very similar to that obtained with configurations prepared using the nonpolarizable RWK2-M water model used previously, provided that the same electron−water pseudopotential is invoked. On the other hand, including the self-consistent many-body potential associated with the water electronic polarizability in the model for the electron−water interaction has a profound effect on the tunneling behavior, making the tunneling probability ∼2 orders of magnitude larger than calculated with the nonpolarizable model. This rectifies the disagreement found before between the tunneling behavior computed with the nonpolarizable water model and experimental results. The strong effect of including the many-body polarizability interactions found in the present study stands in marked contrast to the relatively weak effect found in the context of electron hydration and hydrated electron spectroscopy. The origin of this effect is traced to properties of the lowest excess electron states found for neutral water configurations in the two models: The states associated with the polarizable model are of lower energy yet more extended than the corresponding levels found for the nonpolarizable model. We suggest that the existence of these lower, more extended electronic states in the polarizable model plays a decisive role in the observed lower effective barrier to tunneling through water as compared with vacuum.

1. Introduction

Electron tunneling in condensed molecular environments is a fundamental process which governs many important physical, chemical, and biological phenomena. The study of such processes has therefore been the focus of much experimental and theoretical work for a long time.[1] Two of us have recently carried out a numerical study of electron tunneling through thin water layers confined between two model metal walls.[2] This study has revealed the important role of the discrete three-dimensional structure of the water layer in determing the tunneling probability, demonstrating the inadequacy of continuum dielectric models for quantitative studies of electron transmission in condensed environments. Obviously, however, the results of such model calculations depend on the interaction potentials employed. In the study of ref 2, we applied the same model potentials that were used in earlier studies of electron hydration and of hydrated electron spectroscopy:[3] the flexible RWK2-M water potential[4] and the pseudopotential for the electron−water interaction developed by Barnett et al.[5] A known deficiency of these potentials lies in the fact that the effect of the many-body interaction associated with the electronic polarizability of the water is only partly taken into account—by renormalizing parameters of the two-body interactions so as to fit experimental behavior. This practice works relatively well in reproducing gross features of the structure and the dynamical behavior of liquid water and has been determined to cause errors in the order of 10−15% in the solvation energy and in the lowest excitation energy associated with the hydrated electron.[6] A better representation of the many-body aspect of the solvent polarizability was found to be necessary in MD studies of more subtle issues such as the coordination number in the solvation shell of hydrated ions[7] and the structure of ion−water clusters.[8]

For electron tunneling, the contribution of the electronic polarizability of the medium can be far more important. First, the relative contribution of permanent charge distributions is smaller because tunneling processes are fast relative to characteristic nuclear relaxation times; consequently, the relative contribution of induced charge distributions, which respond on electronic time scales, is larger. Second, variations of the interaction potentials enter exponentially into the tunneling probability. Indeed, simple considerations based on continuum dielectric theory[2] provide partial rationalization to the observed reduction in the effective barrier height (by ∼ 1.2 eV) for electron tunneling through water relative to the corresponding process in vacuum. In contrast, numerical simulations based on the nonpolarizable model yield lower tunneling probability in water relative to vacuum.[2]

In this paper, we investigate the effect of including the interactions associated with the water electronic polarizability on the calculated transmission probability for electron tunneling through water. Two issues are involved: First, including the water polarizability in the intermolecular water−water interaction may affect the resulting water configurations experienced by the tunneling electron. Second, the polarizability response of the water affects the electron−water interaction. Intuitively, we may expect that the second effect is more important, since the available nonpolarizable water potentials have been optimized to yield reliable structures. For the sake of completeness and keeping in mind the exponential sensitivity of the tunneling probability to the barrier structure, we study both effects, albeit separately, in the present paper.

[†] Present address: Department of Chemistry and Biochemistry, University of Texas at Austin, Austin, TX 78712-1167.

[‡] Present address: Department of Chemistry, University of California, Santa Cruz, CA 95064.

[⊗] Abstract published in *Advance ACS Abstracts,* December 1, 1996.

S1089-5639(96)01745-8 CCC: $14.00

In the following section, we discuss our polarizable water model, as well as some basic issues associated with including electronic polarizability in dynamical simulations. We then briefly describe the numerical procedure used to calculate the tunneling probability. Section 4 describes the main numerical results of our work, showing the very significant effect of including the many-body interactions associated with the water polarizability in the calculation. The relation between the resulting transmission probability and the properties of excess electron states in the corresponding bulk medium is also discussed. Section 5 summarizes our conclusions.

2. Polarizable Water Models

As in our previous study,[2] the transmission properties of thin water layers are investigated using static water structures. Now that electronic polarizability is included, this issue warrants extra caution and is discussed below. As before, the water structures are prepared by running classical MD trajectories at 300 K for 192 water molecules in a rectangular box confined in the z direction by two walls, using periodic boundary conditions in the xy plane. The length of the periodic cell in the x and y directions is 23.5 Å, and the distance between the walls is 10 Å. This spacing accommodates three layers of water molecules at normal density. The water−wall interaction is a superposition, for all O and H atoms of 3−9 potentials $V_w = A/d^9 - B/d^3$, where d is the distance from the wall and the parameters A and B are chosen to mimic the water−gold potential.[9] For the water−water interaction, we also use, in addition to the RWK2-M model that was used before, a flexible version of the polarizable SPC (PSPC) model, based on the rigid PSPC model developed and parametrized by Dang.[10]

Consider now the effect of water electronic polarizability in the electron−water pseudopotential. In principle, including the dynamic response of the water electrons with the dynamics of the excess electron amounts to tackling the many-electron aspect of the system. A complete solution of this many-body quantum problem is currently not feasible, and one must resort to approximations based on the relative time scales. A procedure adopted by Staib and Borgis[6a] treats the excess electron on equal footing with the solvent (water) electronic polarizability. These authors use a separable, self-consistent representation in which the polarization charges induced on the water are computed in an electrostatic field which includes the effect of the excess electron charge distribution, while the latter is evaluated self-consistently in the presence of the solvent polarization charges. The nuclear motion is then carried out on a potential hypersurface which represents a ground state for *all* electronic (solvent polarization and excess electron) degrees of freedom. In contrast, Cao and Berne[11] simulate the solvated electron in a polarizable solvent under the assumption that the excitation energy of the former is considerably lower than the electronic excitation energy of the latter. Therefore, the Born−Oppenheimer approximation is invoked by these authors twice: first when evaluating the electronic state of the system, taking the solvated electron as slow relative to the solvent electronic response, and again when moving the even slower nuclei on the potential surface associated with the electronic state obtained in the first step.

In the present calculation, we adopt a viewpoint similar to that of Cao and Berne, in assuming that the tunneling process is *slow* relative to the electronic response of the water molecules. This assumption cannot be justified on general terms, because its validity stems from consideration of relative time scales, and that associated with the tunneling process cannot be uniquely defined for our three-dimensional barriers since no well-defined tunneling path can be identified. The Buttiker−Landauer time[12] for an electron tunneling through a rectangular barrier of height 1 eV and width 10 Å is of the order of 1 fs, while the lowest electronic energy gap of water corresponds to a time scale of ca. 0.1 fs. This shows that situations corresponding to our assumption are possible; however, the time scales are not far enough from each other to make such situations the rule. It is easy to realize that in cases where the barrier electronic response is not immediate on the time scale of the tunneling process, the present approximation will overestimate the effect of water electronic polarizability, and our results should be regarded in this light. It should be emphasized that a separable self-consistent approximation of the type used by Staib and Borgis[6a] is not applicable in the present calculation, because the wave function associated with the transmitted electron becomes strongly fragmented.

3. Numerical Procedure

As mentioned above, the tunneling calculations are done with static water configurations. These configurations are sampled from an equilibrium trajectory for the system described above: 192 water molecules confined between 2 walls separated by 10 Å, with periodic boundary conditions with period 23.5 Å in the directions parallel to the walls, at 300 K, using either the RWK2-M potential or the flexible PSPC model. The new element in the tunneling calculation is the inclusion of the self-consistent effect of the many-body polarizability in the electron−water interaction.

The tunneling probability for an electron between the two walls is calculated, as described in ref 2, by propagating an electron wavepacket through the barrier using the Chebyshev polynomial expansion of the time evolution operator.[13] The water structure is kept frozen in this calculation. The potential barrier experienced by the electron is a superposition of a rectangular barrier of height 5 eV and width 10 Å representing the vacuum barrier and the electron−water interaction. For the latter, we use a modification, described below, of the pseudopotential developed by Barnett et al.[5] that was used successfully in previous studies of electron solvation and of solvated electron spectroscopy in water and in water clusters. The original pseudopotential[5] contains, in addition to Coulomb, exchange and exclusion contributions, terms also associated with the water spherical polarizability, represented by a fictitious polarizable particle of polarizability α located on the oxygen atom. However, only the two-body part of this interaction is taken into account; i.e., the corresponding term in the potential is written for each electron−water pair disregarding the other water molecules. Accordingly, this term has the form

$$V_p(\mathbf{r},\mathbf{R}) = -\frac{0.5\alpha e^2}{[|\mathbf{r}-\mathbf{R}|^2 + R_c^2]^2} \qquad (1)$$

where e is the electron charge, while $\mathbf{r}$ and $\mathbf{R}$ are the positions of the electron and an oxygen atom, respectively. The parameter R_c is a cutoff radius (rationalized by the presence of a strong electron−oxygen repulsion) which eliminates the zero distance singularity in this interaction. The values adopted for α and R_c are 9.745 au (the spherical polarizability of water) and 1.6 au (order of the OH bond length in water), respectively.

In the present evaluation of the electron−water potential, we have retained the same form of the polarizability interaction (i.e., the same term, eq 1, corresponds to the interaction of the electron with a single water molecule); however, we have now determined the overall potential self-consistently; i.e., the corresponding contribution to the potential experienced by the electron at position r is given by[14,15]

$$V_{\mathrm{pol}} = -\frac{1}{2}\sum_j \mu_j \cdot \mathbf{E}_j^{\mathrm{coul}} \tag{2}$$

where $\mathbf{E}_j^{\mathrm{coul}}$ is the electric field at the position of the jth oxygen atom due to the electron

$$\mathbf{E}_j^{\mathrm{coul}} = e\frac{\mathbf{r}_j/|\mathbf{r}_j|}{\tilde{r}_j^{\,2}} \tag{3}$$

and μ_j is the dipole induced on the jth oxygen—the solution of the set of equations

$$\mu_j = \alpha[\mathbf{E}_j^{\mathrm{coul}} - \sum_{k\neq j}\mathbf{T}_{jk}\cdot\mu_k] \tag{4a}$$

$$\mathbf{T}_{jk} = \left(\mathbf{I} - 3\frac{\mathbf{r}_{jk}\cdot\mathbf{r}_{jk}}{|\mathbf{r}_{jk}|^2}\right)\frac{1}{|\mathbf{r}_{jk}|^3} \tag{4b}$$

In eqs 3 and 4, $\mathbf{r}_{jk}$ is the distance vector between the oxygen atoms belonging to the jth and kth water molecules, $\mathbf{r}_j$ is the distance vector from the electron to the jth oxygen atom, and $\tilde{r}_j$ is modified by the cutoff distance; i.e., $\tilde{r}_j^{\,2} = [|\mathbf{r} - \mathbf{R}_j|^2 + R_c^2]$. To simulate the tunneling process, the electron's wave function is evolved on a rectangular 16 × 16 × 1024 grid, with grid spacing 2.77 au in the x and y directions and 0.4 au in the z (i.e., the tunneling) direction. Keeping in line with the assumption that the tunneling dynamics is slow relative to the response of the water electronic polarizability, the polarization induced in the water due to the electrostatic field of the electron and the resulting electrostatic potential at the electron are calculated *at each grid point*, resulting in a modified potential grid for the electron. An example of the resulting potential is seen in Figure 1, which shows the $x-y$ average of the potential $V(x,y,z)$ experienced by the electron in one particular water configuration. The qualitative effect of including the many-body aspect of the water electronic polarizability in obtaining this potential is seen to be a substantial lowering and some smoothing of the xy-averaged potential barrier.

The actual computation of the tunneling probability proceeds as follows (see also ref 2). The initial wavepacket is chosen in the form

$$\psi(\mathbf{r},t{=}0) = Ce^{ik_{x0}x}e^{ik_{y0}y}g(z) \tag{5}$$

where $g(z)$ is centered left to the barrier and contains wavevectors in the positive z direction only. A final time t_f is determined such that the integral of $|\psi(\mathbf{r},t_f)|^2$ over the barrier is smaller than some predetermined small number. The transition probability from an initial free particle state $\mathbf{k}_0$ to a final state $\mathbf{k}_f$ is then obtained from

$$P_{\mathbf{k}_0\rightarrow\mathbf{k}_f} = \frac{|\int \mathrm{d}\mathbf{r}\; e^{-i\mathbf{k}_0\cdot\mathbf{r}}\psi(\mathbf{r},0)|^2}{|\int \mathrm{d}\mathbf{r}\; e^{-i\mathbf{k}_f\cdot\mathbf{r}}\psi(\mathbf{r},t_f)|^2} \tag{6}$$

Since the process is elastic, $|\mathbf{k}_0| = |\mathbf{k}_f|$. The total transmission probability is obtained by summing eq 6 over all final $\mathbf{k}_f$ which satisfy this energy conservation condition together with the condition that their z component is positive. The results shown below correspond to this total transmission probability for an incident $\mathbf{k}_0$ in the z direction, i.e., normal to the barrier.

4. Results and Discussion

Consider first the effect that replacing the nonpolarizable RWK2-M model by a polarizable SPC has on the tunneling probability. In order to check this, we have generated equilibrium MD trajectories using both potential models and have tested several configurations sampled from the two trajectories. As we anticiptated, electron transmission probabilities through the resulting water films, calculated using the same electron−water pseudopotential, are very similar in both cases. In fact, they lie within the statistical range which characterizes an ensemble of such water structures (see Figure 2 below and also Figure 5 of ref 2). This insensitivity to the water intermolecular potential results from the fact that the film structure is determined largely by the confinement imposed by the walls and by the preferred orientation (dipole pointing outwards) of water molecules adjacent to them. Finer details of the intermolecular water interactions make only small effects on the resulting water structures. Keeping this in mind, we disregard this issue in the remainder of our discussion, and the results shown below are all based on configurations prepared using the RWK2-M water model.

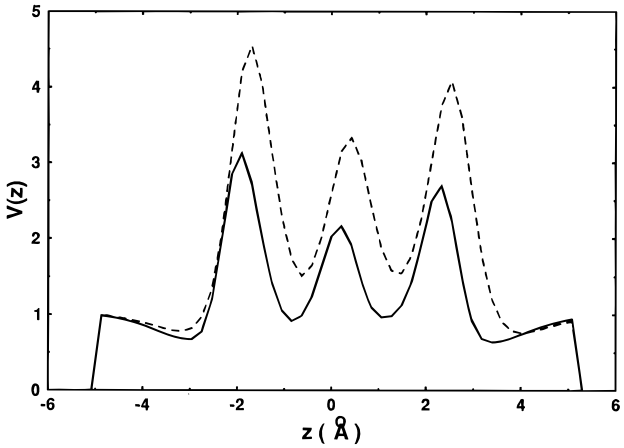

Figure 1. xy-averaged potential barrier. Plotted is $V(z) = (V + V_0)/V_0$, where V is the xy-averaged electron−water potential and V_0 is the bare potential (5 eV, see text). Full line: polarizable model for the electron−water interaction. Dashed line: the nonpolarizable model used in ref 2.

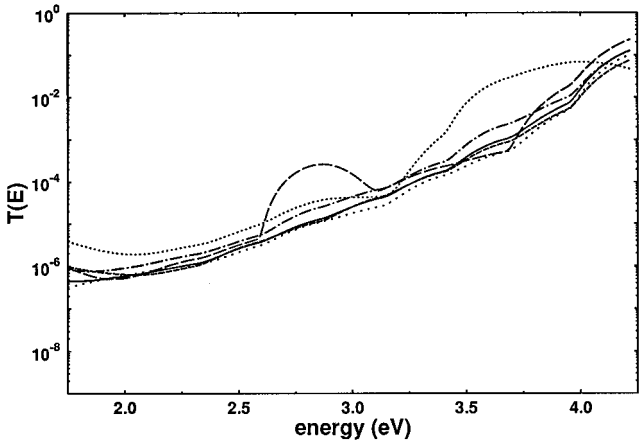

Figure 2. Transmission probability vs electron energy for six equilibrium water configurations, using the polarizable model for the electron−water interaction. The electron is incident in the normal (z) direction, and $T(E)$ denotes the sum over all final directions.

The tunneling probability, as a function of electron energy, through six equilibrium water configurations prepared as described in the previous section is shown in Figure 2. The difference of 0.5−1 order of magnitude in the tunneling probabilities obtained from different configurations seems to be typical of the system studied. This scatter in the results will disappear for larger systems. More important are the qualitative differences between the tunneling behavior in the present model compared with our previous study[2] in which the many-body aspect of the water electronic polarizability response was

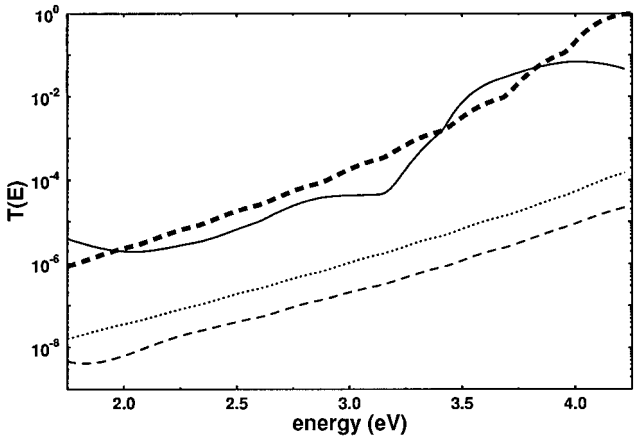

Figure 3. Transmission probability, *T(E)*, averaged over six equilibrium water configurations as described in the text. Full line: using the polarizable model. Thin dashed line: using the nonpolarizable model of ref 2. Also shown are the transmission probabilities through a rectangular barrier of height = 5 eV, which corresponds to the model vacuum barrier (dotted line), and through a rectangular barrier of height 3.8 eV (thick dashed line).

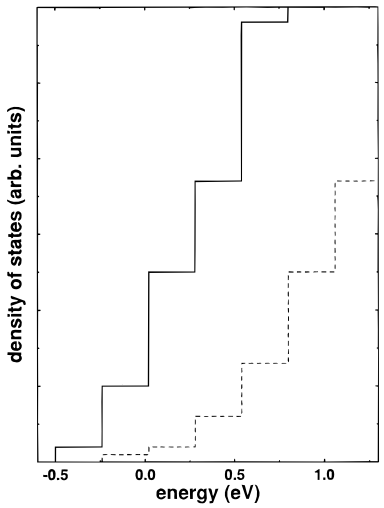

Figure 4. Histogram plot of the density of levels for an excess electron in a neutral "bulk" water configuration. Full line: polarizable model. Dashed line: nonpolarizable model.

disregarded. First, the tunneling probabilities obtained here are ∼2 orders of magnitudes higher than in the previous study. Second, unlike in that study, some configurations now support resonances, as signaled by the corresponding peaks in the tunneling probability vs energy plots.

A clearer picture of the difference between the two electron−water interaction models with regard to the tunneling behavior is seen in Figure 3. Here we show, as functions of the incident electron energy, the averaged (over eight configurations) electron-through-water tunneling probabilities in the models which take (full line) or do not take (thin dashed line) into account the many-body aspect of the water electronic polarizability. Also shown are the corresponding results (dotted line) for tunneling through vacuum, i.e., through a bare rectangular potential barrier of height 5 eV, and a similar result (thick dashed line) for a barrier of 3.8 eV which corresponds to the expected lowering of the effective barrier for tunneling through water. The results for the polarizable model are seen to be in remarkable agreement with the expectation based on lowering of the effective rectangular barrier by 1.2 eV.

Figure 3 shows that taking into account the full many-body character of the water electronic polarizability is crucial in the present context. The effect of water on the tunneling behavior is associated with several factors: First, the fact that much of the physical space between the electrodes is occupied by oxygen atom cores which are practically impenetrable to the electron forces the tunneling to take relatively long winding pathways rather than the shortest path perpendicular to the electrodes. This makes the tunneling less probable; namely, the effective barrier for tunneling is higher. Second, the ordering of the water molecules at the metal walls, with the negative oxygen sites nearest to the wall and a net positive dipole pointing away from the surface, amounts to a surface dipole layer which reduces the electrode work function, i.e., the effective barrier to tunneling. We have studied this effect in ref 2 within the nonpolarizable water model and have found that when the specific oxygen−wall attraction is eliminated from the water−wall model potential, the tunneling probability in a system of the type studied here decreases by 0.5−1 order of magnitude.

Finally, the properties of excess electron states in the polarizable water environment can also affect the transmission properties of this medium. We focus on low energy states of an excess electron in equilibrium configurations of bulk neutral water. Such states may be weakly bound ("preexisting localized state" in discussions of electron solvation) or unbound. The lowest extended states correspond to what is sometimes referred to as "the bottom of the water conduction band". The latter is believed to lie ∼1 eV below vaccum energy; however, nonpolarizable water models put this energy at ∼0 relative to vacuum.[16] Obviously, a low-lying conduction band implies a lower effective potential barrier for electron tunneling.

In Figure 4, we compare the density of excess electron states as a function of energy, for the nonpolarizable and for the polarizable water models described in Section 2. In these calculations, we have used "bulk" water configurations sampled from an equilibrium MD trajectory for 192 water molecules in a simulation cube of size (17.56 Å)^3 (density 1 g/cm^3) with minimum image convention and at 300 K. The low-energy eigenvalues of an excess electron in the resulting water configurations were calculated on a 16 × 16 × 16 grid with grid spacing 2.11 au, using a block Lanczos algorithm. The accuracy of the results shown in Figure 4 is not high, because only 10 water configurations were used. However, the difference between the polarizable and the nonpolarizable model is evident: The band of excess electron states in the nonpolarizable water model starts essentially at $E = 0$ (relative to vacuum), similar to what was seen in ref 16 using a somewhat different nonpolarizable model. In contrast, using the same water configurations with the electron−water interaction modified to take into account the many-body aspects of the water electronic polarizability leads to a band edge at ∼−0.5 eV relative to vacuum. Another source of error in this determination of the band edge is the fact that for the polarizable model, the corresponding electron wave functions are of spatial size comparable to or larger than our grid. This implies that the computed energies are higher than the actual ones and that the values of −0.5 eV is, in fact, an upper limit.

Because the spatial spread of the eigenfunctions associated with the low-energy excess electron states in the polarizable water model is comparable to the grid size used, it was not possible to determine whether these states are localized or extended (obviously, no finite grid calculation can unquestionably determine that a state is extended). This is, however, of little importance to our discussion, since it is sufficient to assert that a state is extended enough to span the space between the electrodes. It is interesting to compare the polarizable and the nonpolarizable models with respect to this issue. Figure 5 compares the spread of the eigenfunctions associated with the eigenenergies used to generate the densities of Figure 4. Plotted in Figure 5 are the "entropies"

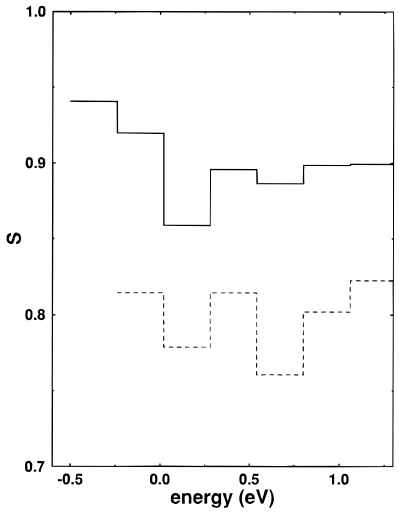

Figure 5. Histogram plot of the "entropy" function, eq 7, for the electronic states of the polarizable (full line) and nonpolarizable (dashed line) models.

$$S = -\frac{\sum_{j=1}^{N} |\psi_j|^2 \ln|\psi_j|^2}{\ln N} \qquad (7)$$

where the sum is over all grid points. This function measures the extent of the spatial dispersion of the corresponding wave function. It becomes unity when the electron is equally likely to be at any grid point, i.e., if $|\psi_j|^2 = 1/N$, where N is number of grid points (here 16^3), and is zero if the electron is located in one particular grid point k, i.e., $|\psi_j|^2 = \delta_{jk}$. It is clear from Figure 5 that the electron wave functions associated with the low-energy states of the polarizable water model are considerably more extended than the corresponding states in the nonpolarizable model. This may be another factor affecting the electron tunneling probability. The combined effect of all these factors, the expulsion of the electron from the oxygen cores, the effect of ordered surface water on the work function, and the properties of excess electron states in neutral water, combine to yield the overall reduction in the effective barrier to tunneling, which leads to the strongly enhanced tunneling probability seen in the polarizable model (Figure 3).

5. Summary and Conclusions

In this paper, we have examined the effect of including the water electronic polarizability in the force fields which determine electron tunneling through water layers. First, we have prepared water equilibrium configurations by sampling from MD trajectories obtained with the flexible version of the PSPC potential for water due to Dang.[10] We have found that tunneling through these configurations behaves very similarly to our previous results which use configurations obtained with the nonpolarizable RWK2-M water potential. We have concluded that in the confined geometry of water between the two walls, finer details of the water structure which are determined by the intermolecular water potential make little difference on the resulting water structure.

We have also incorporated the many-body aspect of the water electronic polarizability response into the electron−water interaction and examined its effect on the effective barrier for tunneling of an electron through thin layers of water. Strictly speaking, the potential used in our study is inadequate for quantitative computations, because we have introduced this extra feature into the electron−water interaction without reparametrizing the whole pseudopotential, so our results should be regarded only as qualitative indications. For example, we have found that changing the parameter R_c of eq 1 from 1.6 to 1.8 changes the resulting tunneling probability by a factor of ∼2−3, while the effect of interest here is the increase by 2 orders of magnitudes of the tunneling probability in the polarizable water model relative to the nonpolarizable model.

This substantial increase in the tunneling probability through water described by the polarizable model for the electron−water interaction changes qualitatively the picture which emerged from our previous calculation:[2] The tunneling probability through a thin layer (10 Å) of water is found to be larger by more than an order of magnitude than the corresponding value in vacuum, in accord with expectations for lowering an effective rectangular barrier by 1−1.5 eV. The physical origin of this effect has been determined to be the combination of three factors: The effective increase in the barrier height associated with the insurmountable oxygen cores is more than compensated by the effective decrease in the barrier caused by the lowering of the metal work function due to the ordering of the water dipoles at the surface and to the existence of "conducting" states below the vacuum energy in the barrier.

The use of static water configurations in the present study was a highly simplifying feature which seemed to be justifiable in the circumstances studied. However, it is important to keep in mind that the dynamics of the barrier electronic and nuclear response may be important in electron tunneling processes. This issue will be considered in future work.

Acknowledgment. The research of A. N. is supported by grants from the USA−Israel Binational Science Foundation and from the Israel Ministry of Science. I. B. acknowledges support from the Petroleum Research fund, administered by the American Chemical Society, and the NSF. P. G. is thankful to the Minerva−Stiftung for a postdoctoral fellowship.

References and Notes

(1) See, e.g., Wolf, E. L. *Principles of Electron Tunneling Spectroscopy*; Oxford University: New York, 1985. DeVault, D. *Quantum Mechanical Tunneling in Biological Systems*; Cambridge University: Cambridge, 1984.
(2) Mosyak, A.; Nitzan, A.; Kosloff, R. *J. Chem. Phys.* **1996**, *104*, 1549.
(3) Barnett, R. N.; Landman U.; Nitzan, A. *J. Chem. Phys.* **1988**, *89*, 2242; **1989**, *90*, 4413; **1989**, *91*, 5567; **1990**, *93*, 6535, 8187. Barnett, R. N.; Landman, U.; Rajagopal, G.; Nitzan, A. *Israel J. Chem.* **1990**, *30*, 85. Barnett, R. N.; Landman, U.; Makov, G.; Nitzan, A. *J. Chem. Phys.* **1990**, *93*, 6226. Neria, E.; Nitzan, A.; Barnett, R. B.; Landman, U. *Phys. Rev. Lett.* **1991**, *67*, 1011.
(4) Reimer, J. R.; Watts, R. O.; Klein, M. L. *Chem. Phys.* **1982**, *64*, 95. Reimer, J. R.; Watts, R. O. *Chem. Phys.* **1984**, *85*, 83.
(5) Barnett, R. N.; Landman, U.; Cleveland, C. L. *J. Chem. Phys.* **1988**, *88*, 4420.
(6) (a) Staib, A.; Borgis, D. *J. Chem. Phys.* **1995**, *103*, 2642. (b) Schweighofer, K. J.; Benjamin, I. To be submitted. (c) Nitzan, A.; Landman U. Unpublished results.
(7) (a) Sprik, M.; Klein, M. L.; Watanabe, K. *J. Phys. Chem.* **1990**, *94*, 6483. Sprik, M. *J. Phys. Chem.* **1991**, *95*, 2283. (b) Dang, L. X.; Rice, J. E.; Caldwell, J.; Kollman, P. A. *J. Am. Chem. Soc.* **1991**, *113*, 2481.
(8) Perera, L.; Berkowitz, M. L. *J. Chem. Phys.* **1991**, *95*, 1954.
(9) Hautman, J.; Halley, J. W.; Rhee, Y.-J. *J. Chem. Phys.* **1989**, *91*, 467.
(10) Dang, L. X. *J. Chem. Phys.* **1992**, *97*, 2659.
(11) Cao, J.; Berne, B. J. *J. Chem. Phys.* **1993**, *99*, 2902.
(12) Buttiker, M.; Landauer, R. *Phys. Rev. Lett.* **1982**, *49*, 1739; *Phys. Scr.* **1985**, *32*, 429.
(13) Tal-Ezer, H.; Kosloff, R. *J. Chem. Phys.* **1984**, *81*, 3967.
(14) Perera, L.; Amar, F. G. *J. Chem. Phys.* **1989**, *90*, 7354.
(15) Kistenmacher, H.; Lie, G. C.; Popkie, H.; Yoshmine, M. *J. Chem. Phys.* **1974**, *61*, 546.
(16) Motakabbir, K. A.; Rossky, P. J. *Chem. Phys.* **1989**, *129*, 253.